

Light clusters in nuclear matter of finite temperature

M. Beyer, S. Strauss¹, P. Schuck², and S.A. Sofianos³

¹ Fachbereich Physik, Universität Rostock, D-18051 Rostock, Germany

² Institut de Physique Nucléaire, F-91406, Orsay Cedex, France

³ Physics Department, University of South Africa, Pretoria 0003, South Africa

Received: date / Revised version: date

Abstract. We investigate properties and the distribution of light nuclei ($A \leq 4$) in symmetric nuclear matter of finite temperature within a microscopic framework. For this purpose we have solved few-body Alt-Grassberger-Sandhas type equations for quasi-nucleons that include self-energy corrections and Pauli blocking in a systematic way. In a statistical model we find a significant influence in the composition of nuclear matter if medium effects are included in the microscopic calculation of nuclei. If multiplicities are frozen out at a certain time (or volume), we expect significant consequences for the formation of light fragments in a heavy ion collision. As a consequence of the systematic inclusion of medium effects the ordering of multiplicities becomes opposite to the law of mass action of ideal components. This is necessary to explain the large abundance of α -particles in a heavy ion collision that are otherwise largely suppressed in an ideal equilibrium scenario.

PACS. 25.70.-z Low and intermediate energy heavy-ion reactions – 25.70.Pq Multifragment emission and correlations – 21.65.+f Nuclear matter – 21.45.+v Few-body systems

1 Introduction

Heavy ion collisions provide a tool to investigate the phase structure of nuclear matter. Depending on the energies, the region of temperature and density explored might be rather large. The information about the composition of nuclear matter is contained in the equation of state. At collision energies per nucleon well below one GeV the equation of state is described by purely hadronic degrees of freedom. It is a basic ingredient in microscopic simulations of the heavy ion collision, such as the Boltzmann-Uehling-Uhlenbeck (BUU) [1,2,3,4,5] or the quantum molecular dynamics (QMD) [6,7,8] simulations. The challenge is to extract information about the different stages of the evolution of the heavy ion collision. This information could be provided by fragments produced in the different stages of the collision as has been done recently for the case $^{129}\text{Xe} + ^{\text{nat}}\text{Sn}$ by the INDRA collaboration [9,10].

An early analysis of multi-fragmentation in a heavy ion collision of $^{36}\text{Ar} + ^{58}\text{Ni}$ at several energies below 100A MeV has been given in Ref. [11]. The authors study a class of evaporation events at central collisions [12]. During these events more than 90% of the charged particles were detected and isotopically identified. Within a thermal (and chemical) equilibrium scenario [13] of ideal gas components (including states up to excited ^9B), supplemented by finite volume effects [14] and a model of side-feeding, they found a remarkable agreement with the experimental data [11]. Temperature has been varied between 10 and

25 MeV and the freeze-out volume fixed to 1/3 of normal nuclear matter density.

A more elaborated statistical analysis has been done for the recent INDRA experiment $^{129}\text{Xe} + ^{\text{nat}}\text{Sn}$. The measured multiplicities of the central collisions by the INDRA collaboration show a large fraction of α -particles [10]. In contrast, a naive model of a gas of ideal components, would give a much smaller number of α -particles, depending on the freeze-out density. The INDRA collaboration provides a detailed comparison of their data within a statistical multi-fragmentation model (SMM) [15]. This model goes beyond a simple picture of an ideal gas and describes multiplicities and some other aspects of the heavy ion collision in question [10].

On the other hand, from a microscopic analysis of cluster formation, it is known that nuclei dissociate already at rather moderate densities and temperatures, see, e.g. [16, 17] and references therein. Some details will also be given in this paper. The dissociation (Mott effect) is taken into account, e.g., in modern BUU simulations of heavy ion collisions and is necessary to reproduce the experimental data, see Ref. [1,2]. It is an effect related to the Pauli blocking induced by the surrounding medium and goes beyond the picture of a simple ideal gas of nuclei.

In a recent analysis of the central collision $\text{Xe} + \text{Sn}$ at 50A MeV that has been measured by the INDRA collaboration [9], we found that the BUU simulation gives a proton to deuteron ratio that is close to the one expected by the equilibrium distribution; to be more precise, for times

$t > 50 \text{ fm}/c$ during the evolution of the system. This however holds only, if the equilibrium distribution includes the above mentioned dissociation of the deuteron [5, 18].

Therefore, we address the question to what extend the dissociation of nuclei affects the equilibrium distribution of nuclear matter. To do so, we investigate a system of light nuclei at finite density and temperature up to the α -particle.

Hence, we focus on a new aspect in the distribution of light nuclei. Since reasonable generalizations of the Feynman-Galitskii or Bethe-Goldstone equations for more than two particles become available, the properties of multi-particle correlations in a medium can now be addressed microscopically. To demonstrate the effect that is related to in-medium properties of the light clusters in question, in particular the α -particle, we explore an *ab initio* equilibrium quantum statistical description of a many-particle system based on the well established and successful (equilibrium) Green function method [19]. To include a proper description of clusters we implement an equal time constraint on the Green functions. This allows for a cluster expansion of the Green functions as shown, for example in [20]. In an uncorrelated medium of quasi-particles the equal time constraint systematically leads to Dyson equations for clusters with a fixed number of particles. They include the self energy corrections and the Pauli blocking and are rearranged as resolved equations to use the Alt-Grassberger-Sandhas (AGS) formalism to solve the respective few-body equations which has been done for the three- and four-nucleon system in [21, 16, 17]. Similar equations to treat the in-medium three-body system have been proposed previously in Refs. [23, 24]. As an interaction we use a nucleon nucleon potential that reasonably reproduces the nucleon nucleon phase shifts and the binding energies of the light nuclei in question.

In Section 2 we introduce the consequences of the above-mentioned cluster expansion method in the equation of state. This will be done along the lines of [25]. The microscopic AGS-type equations to treat multi-particle clusters in medium will be explained in Section 3. We use a nucleon-nucleon potential that reproduces reasonably well the nucleon-nucleon scattering data and the binding energies of light nuclei considered. In Section 4 we present our results. In particular, we calculate the equilibrium composition of nuclear matter for conditions comparable to the heavy ion collision investigated by the INDRA collaboration. We summarize our conclusions in Section 5.

2 Statistical model

To generalize the equation of state for a Fermi system that includes correlations the nuclear matter density $n = n(\mu, T)$ as a function of the chemical potential μ and temperature T can be rearranged in an uncorrelated part n_{free} and a correlated one n_{corr} [25, 16],

$$n = n_{\text{free}} + n_{\text{corr}}. \quad (1)$$

To abbreviate notation let 1 denote the quantum numbers of particle 1. The Fermi function is given by

$$f(1) \equiv f(E_1) = \{\exp[\beta(E_1 - \mu)] + 1\}^{-1} \quad (2)$$

where E_1 denotes the one-particle energy and β the inverse temperature. Presently we describe symmetric nuclear matter and hence

$$n_{\text{free}} = 4 \sum_1 f(1). \quad (3)$$

For a system of nucleons of mass m_N the energy is $E_1 = k^2/2m_N$. Hartree-Fock approximation introduces the notion of quasi-particles and quasi-particle energies

$$E_1 \rightarrow \varepsilon_1 = k^2/2m_N + \Sigma(k), \quad (4)$$

where

$$\Sigma(1) = \sum_2 V_2(12, \tilde{12})f(2). \quad (5)$$

The tilde means proper anti-symmetrization (i.e. including the Fock term).

As explained in Ref. [16] in some detail, the correlated density can be composed into different cluster contributions.

$$n_{\text{corr}} = 2n_2 + 3n_3 + 4n_4 + \dots, \quad n_A = n_A^b + n_A^s \quad (6)$$

where n_A denotes the A -particle correlated density presented as bound n_A^b or scattering n_A^s states in chemical equilibrium. The full expression for the two-particle correlated densities n_2 has been given in Ref. [25].

To evaluate correlated densities we presently focus on the bound state contributions. This is justified in view of the rather low densities of the final stage of heavy ion collisions. Note, however, that including contributions of scattering states requires major theoretical effort to solve the respective scattering few-body equations derived in the next section. The distribution functions for the A -body cluster of fermions is given by

$$f_A(p) = \{\exp[\beta(E_A - B_A - \mu_A)] + \epsilon\}^{-1} \quad (7)$$

where p is the c.m. momentum of the cluster, $E_A(p)$ is the continuum energy, $B_A > 0$ the binding energy of the cluster, $\epsilon = +1(-1)$ for fermions (bosons), and μ_A the respective chemical potential. In equilibrium considered here $\mu_A = A\mu$. The density for the nucleus of mass number A is given by

$$n_A^b(\mu, T) = (2S + 1)(2I + 1) \sum_p f_A(p) \quad (8)$$

where S denotes the spin and I the isospin of the nucleus.

3 In-medium few-body equations

The basis of the equations given in this section is the (equilibrium) Green function approach to describe quantum

statistical systems [19]. The Green functions for a given number of particles are evaluated at equal imaginary times assuming an environment of independent quasi-particles, see e.g. [20]. As a consequence, for a given number of particles, a Dyson-type equation can be derived that is only driven by the dynamics of the smaller cluster (cluster mean field approximation) that breaks the Green functions hierarchy. Utilizing resolvents the Dyson-type equation for a particular cluster can be rewritten as AGS-type equation [26, 27, 28, 29] with an effective Hamiltonian. This has been shown previously for the nucleon deuteron reaction [21] the three-nucleon bound state [16] and the α -particle [17]. In this section we briefly repeat the relevant formulas to introduce our notation.

Utilizing the Dyson equation for clusters it is possible to introduce resolvents to describe the dynamics of the system. Defining $H_0 = \sum_{i=1}^n \varepsilon_i$, with the quasi-particle self energy ε_i the n -quasi-particle cluster resolvent G_0 is

$$G_0(z) = (z - H_0)^{-1} N \equiv R_0(z) N. \quad (9)$$

Here G_0 , H_0 , and N are matrices in n particle space and z denotes the analytic continuation of the Matsubara frequency [19]. The Pauli-blocking factors for n -particles are

$$N = \bar{f}(1)\bar{f}(2)\dots\bar{f}(n) + \epsilon f(1)f(2)\dots f(n), \quad (10)$$

with $\bar{f} \equiv 1 - f$. Note: $NR_0 = R_0N$. Defining the effective potential $V \equiv \sum_{\text{pairs } \alpha} N_2^\alpha V_2^\alpha$ the full, $G(z)$, and the channel, $G_\alpha(z)$, resolvents are

$$G(z) = (z - H_0 - V)^{-1} N \equiv R(z)N, \quad (11)$$

$$G_\alpha(z) = (z - H_0 - N_2^\alpha V_2^\alpha)^{-1} N \equiv R_\alpha(z)N. \quad (12)$$

Note that $V^\dagger \neq V$ and $R(z)N \neq NR(z)$. For the scattering problem it is convenient to define the in-medium AGS operator $U_{\beta\alpha}(z)$ [21]

$$R(z) = \delta_{\beta\alpha} R_\beta(z) + R_\beta(z) U_{\beta\alpha}(z) R_\alpha(z) \quad (13)$$

that after some algebra leads to the in-medium AGS equation

$$U_{\beta\alpha}(z) = \bar{\delta}_{\beta\alpha} R_0(z)^{-1} + \sum_\gamma \bar{\delta}_{\beta\gamma} N_2^\gamma T_2^\gamma(z) R_0(z) U_{\gamma\alpha}(z), \quad (14)$$

where $\bar{\delta}_{\beta\alpha} \equiv 1 - \delta_{\beta\alpha}$. The square of this AGS-operator is directly linked to the differential cross section for the scattering process $\alpha \rightarrow \beta$, for all Fermi functions $f(i) \rightarrow 0$. Hence the isolated three-body system is recovered. The driving kernel consists of the two-body t -matrix derived in the same formalism, however given earlier and known as Feynman-Galitskii (finite T) or Bethe-Goldstone ($T = 0$) equations [19, 22]

$$T_2^\gamma(z) = V_2^\gamma + V_2^\gamma N_2^\gamma R_0(z) T_2^\gamma(z).$$

A numerical solution of the three-body break-up reaction relevant for the chemical distribution in a heavy ion collision using a coupled Yamaguchi potential has been given in Ref. [21].

For the bound state problem it is convenient to introduce form factors

$$|F_\beta\rangle = \sum_\gamma \bar{\delta}_{\beta\gamma} N_2^\gamma V_2^\gamma |\psi_{B_3}\rangle. \quad (15)$$

Since the potential is non symmetric, the right and left eigenvectors are different, although the bound state energies are the same. The eigenvectors are explicitly needed in our solution of the four-body system. The respective homogeneous AGS equations are given by

$$|F_\alpha\rangle = \sum_\beta \bar{\delta}_{\alpha\beta} N_2^\beta T_2^\beta(B_3) R_0(B_3) |F_\beta\rangle, \\ |\tilde{F}_\alpha\rangle = \sum_\beta \bar{\delta}_{\alpha\beta} T_2^\beta(B_3) N_2^\beta R_0(B_3) |\tilde{F}_\beta\rangle. \quad (16)$$

We now turn to the four-body problem in matter. In addition to having different channels as for the three body system now the channels appear in different partitions that makes the four-body problem even more involved. The partitions of the four-body clusters are denoted by $\rho, \tau, \sigma, \dots$, e.g., $\rho = (123)(4), (234)(1), \dots$ for 3 + 1-type partitions, or $\rho = (12)(43), (23)(41), \dots$ for 2 + 2-type partitions. The two-body sub-channels are denoted by pair indices $\alpha, \beta, \gamma, \dots$, e.g. pairs (12), (24), ... The two- and three-body t -matrices have to be defined with respect to the partitions that leads to additional indices. A convenient way to solve the four-body in-medium homogeneous AGS equation is by introducing form factors

$$|\mathcal{F}_\beta^\sigma\rangle = \sum_\tau \bar{\delta}_{\sigma\tau} \sum_\alpha \bar{\delta}_{\beta\alpha}^{\tau\sigma} R_0^{-1}(B_4) |\psi_{B_4}\rangle, \quad (17)$$

where $\bar{\delta}_{\beta\alpha}^{\tau\sigma} = \bar{\delta}_{\beta\alpha}$, if $\beta, \alpha \subset \tau$ and $\bar{\delta}_{\beta\alpha}^{\rho} = 0$ otherwise and $|\psi_{B_4}\rangle$ is the α -particle in-medium wave function. The homogeneous equations then read [17]

$$|\mathcal{F}_\beta^\sigma\rangle = \sum_{\tau\gamma} \bar{\delta}_{\sigma\tau} U_{\beta\gamma}^\tau(B_4) R_0(B_4) N_2^\gamma T_2^\gamma(B_4) R_0(B_4) |\mathcal{F}_\gamma^\tau\rangle, \quad (18)$$

where $\alpha \subset \sigma, \gamma \subset \tau$. A numerical solution of this equation is rather complex. In order to reduce computational time, needed in particular to handle the dependence on the medium, we introduce an energy dependent pole expansion (EDPE) that has been proven useful in many applications involving the α -particle and is accurate enough for the present purpose [30]. However, we have to generalize the original version of the EDPE because of different right and left eigenvectors appearing for the three-body subsystem and given in Eq. (16) (for details see [17]).

In the *two-body* sub-system the EDPE reads

$$T_\gamma(z) \simeq \sum_n |\tilde{F}_{\gamma n}(z)\rangle t_{\gamma n}(z) \langle \tilde{F}_{\gamma n}(z)| \\ \simeq \sum_n |\tilde{g}_{\gamma n}(z)\rangle t_{\gamma n}(z) \langle g_{\gamma n}| \\ = \sum_n N_2^\gamma |g_{\gamma n}\rangle t_{\gamma n}(z) \langle g_{\gamma n}|. \quad (19)$$

where we have chosen a Yamaguchi ansatz for the form factors for simplicity. The last line shows the explicit dependence of the Pauli blocking factors. Inserting this ansatz into the Feynman-Galitskii equation determines the propagator $t_{\gamma n}(z)$. In the *three-body* sub-system the EDPE expansion reads

$$\langle g_{\beta m}(z) | R_0(z) U_{\beta\gamma}^\tau(z) R_0(z) | \tilde{g}_{\gamma n}(z) \rangle \simeq \sum_{t,\mu\nu} \langle \tilde{I}_{\beta m}^{\tau t,\mu}(z) \rangle t_{\mu\nu}^{\tau t}(z) \langle \Gamma_{\gamma n}^{\tau t,\nu}(z) \rangle. \quad (20)$$

with the three-body EDPE functions

$$|\tilde{I}_{\beta m}^{\tau t,\mu}(z)\rangle = \langle g_{\alpha n}|R_0(z)|\tilde{g}_{\beta m}\rangle t_{\beta m}(B_3)|\tilde{I}_{\beta m}^{\tau t,\mu}\rangle, \quad (21)$$

that we get from solving the following Sturmian equations

$$\eta_{t,\mu}|\tilde{I}_{\alpha n}^{\tau t,\mu}\rangle = \sum_{\beta m} \langle g_{\alpha n}|R_0(B_3)|\tilde{g}_{\beta m}\rangle t_{\beta m}(B_3)|\tilde{I}_{\beta m}^{\tau t,\mu}\rangle \quad (22)$$

$$\eta_{t,\mu}|\Gamma_{\alpha n}^{\tau t,\mu}\rangle = \sum_{\beta m} \langle \tilde{g}_{\alpha n}|R_0(B_3)|g_{\beta m}\rangle t_{\beta m}(B_3)|\Gamma_{\beta m}^{\tau t,\mu}\rangle \quad (23)$$

Inserting the EDPE into the homogeneous AGS equations allows us to redefine the form factors that are now operators depending on the coordinates of the $2+2$ or $3+1$ system, i.e.

$$|\Gamma_\nu^{\sigma s}\rangle = \sum_{\beta m} \langle \Gamma_{\beta m,\nu}^{\sigma s}(B_4) | t_{\beta m}(B_4) \langle g_{\beta m}(B_4) | R_0(B_4) | \mathcal{F}_\beta^\sigma \rangle \rangle \quad (24)$$

and therefore the final homogeneous equation

$$|\Gamma_\mu^{\sigma s}\rangle = \sum_{\tau t} \sum_{\nu\kappa} \sum_{\gamma n} \bar{\delta}_{\sigma\tau} \langle \Gamma_{\gamma n}^{\sigma s,\nu}(B_4) | t_{\gamma n}(B_4) | \tilde{I}_{\gamma n}^{\sigma s,\mu}(B_4) \rangle \times t_{\mu\kappa}^{\tau t}(B_4) |\Gamma_\kappa^{\tau t}\rangle, \quad (25)$$

is an effective one-body equation with an effective potential \mathcal{V} and an effective resolvent \mathcal{G}_0 defined as

$$\mathcal{V}_{\mu\nu}^{\sigma s,\tau t}(z) = \sum_{\gamma n} \bar{\delta}_{\sigma\tau} \langle \Gamma_{\gamma n}^{\sigma s,\mu}(z) | t_{\gamma n}(z) | \tilde{I}_{\gamma n}^{\sigma s,\nu}(z) \rangle, \quad (26)$$

$$\mathcal{G}_{\mu\nu,0}^{\sigma s,\tau t}(z) = t_{\mu\nu}^{\tau t}(z). \quad (27)$$

4 Results

4.1 Cluster properties

The binding energies of the few-nucleon systems depend on the chemical potential μ or equivalently the density $n(\mu, T)$, the temperature T , and c.m. momentum $P_{\text{c.m.}}$. For the two-, three-, and four-nucleon systems the binding energies are shown in Fig. 1 for $T = 10$ MeV and $P_{\text{c.m.}} = 0$ [17]. The line $B_A = 0$ reflects the respective continuum threshold. We mention here that the medium dependence of the binding energies is rather similar for different two-body potentials, although their results for the isolated system may be very different for the few-nucleon

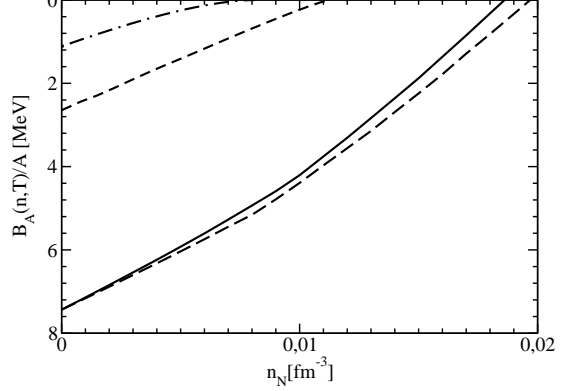


Fig. 1. Density dependence of the binding energy per nucleon of deuterons (dash-dot), Triton (dashed), and α -particle with Malfliet Tjon potential (solid), Yamaguchi potential (long-dashed) at $P_{\text{c.m.}} = 0$, as given in Ref. [17].

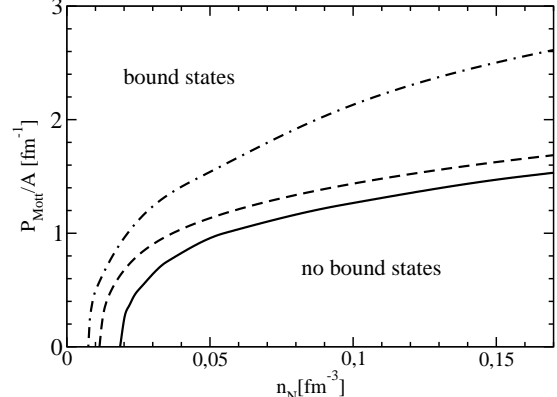


Fig. 2. Momenta per nucleon as a function of the dissociation density for deuteron (dash-dot), triton (dash), α -particle (solid). Bound states exist only above the respective lines.

systems considered. This has been mentioned earlier, but it can also be seen from the two lines representing different potentials for the α -particle, i.e. Yamaguchi [31] (long dashed) and Malfliet-Tjon potential [32] (solid) after renormalizing the binding energies to the same value of the MTI-III potential. For ${}^3\text{He}$ that is not shown in Fig. 1 the dissociation density is slightly smaller due to the Coulomb force that has been evaluated perturbatively. However, for asymmetric nuclear matter, e.g. $N_p/N_n \simeq 0.72$ (for the ${}^{129}\text{Xe} + {}^{119}\text{Sn}$ reaction) this effect is compensated [33].

Because of the medium the pole of the bound state moves to the continuum threshold as seen in Fig. 1. The bound state vanishes because of the quasi-particle nature of the cluster. However, investigating the zeros of the two-body Jost function we found earlier that the quasi deuteron “survives” as a virtual bound state with different energies, depending on the densities above the dissociation line [34]. This is a similar state as the virtual 1S_0 nucleon nucleon state at 70 keV. This means that the quasi deuteron retains its quasi-particle nature of being an infinitely long living state and does not become a

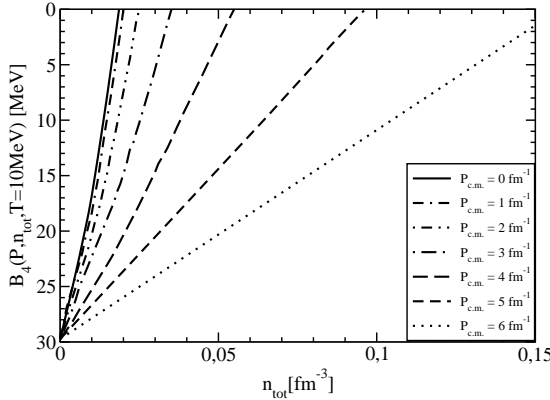


Fig. 3. Density dependence of the binding energy of the α -particle for finite $P_{\text{c.m.}}$ as indicated in the legend.

resonance. Only going beyond the quasi-particle picture the deuteron spectral function will acquire an imaginary part and hence the deuteron becomes a state of finite life time in the medium. This is due to break-up processes in nuclear matter, the simplest one being the three-nucleon reaction [21]. Such an investigation for three- and four-body system is also technically involved and still needs to be done.

Also a possible appearance of Efimov states related to $B \rightarrow 0$ of the sub-system needs further investigation [35]. Since the Efimov states are 'excited' states, e.g. for the three-body system they are close to the $2 + 1$ threshold, their blocking may be smaller since the wave functions contain higher momentum components, hence the slope of their dependence on the density is flatter. Also, as seen from Fig. 1, the slope of the binding energies as a function of densities for the larger clusters is steeper. On the other hand the sub-system is not at rest in the larger cluster, hence the binding energy changes, as we will show in the next paragraph, and therefore a careful analysis is needed that would go beyond the present scope of the paper. Hence so far no conclusion can be drawn for the appearance of Efimov states, but it is an important issue since Efimov states might effect the equation of state for clustering Fermi systems.

For a finite c.m. momentum relative to the medium (at rest) the influence of the medium is weaker, as less components of the wave functions are blocked by the Fermi sea. For deuteron [36] and triton [16] this has been given in earlier references, see also references therein. In Fig. 3 we give the results for the α -particle. Note again that the medium effects do not change the elementary property of an α -particle, however, after introducing effective degrees of freedom, the α -particle and any other cluster considered here consists of quasi-nucleons and not elementary nucleons. Besides the change of nucleon self energy also the binding energy of the cluster is changed and hence the clusters can be viewed as quasi-deuterons, quasi-tritons, quasi- α 's, etc., i.e. clusters with the respective self-energy corrections.

For a given temperature, here we chose $T = 10$ MeV, the momentum of dissociation P_{dis} is defined by the condition

$$B(n_{\text{dis}}, T, P_{\text{dis}}) = 0, \quad (28)$$

i.e., the density n_{dis} and the momentum P_{dis} where binding of the nucleons is lost. For a system of atoms and ions this scenario can be related to a transition of an isolator to a conductor, since electrons can move away from the ion because of the dissociation property. The respective dissociation lines for deuterons, tritons/ ^3He , and α -particles are shown in Fig. 2. The momentum is normalized to the number of nucleons in the cluster that is identical to the velocity of the cluster on the dissociation line.

4.2 Cluster distribution

We now consider the composition of nuclear matter in equilibrium at a temperature of $T = 10$ MeV. To this end we assume that nuclear matter is composed of nucleons, deuterons, tritons, ^3He , and α -particles. Larger clusters are presently not considered. We investigate three scenarios:

- gas of nucleons and nuclei with all properties of the isolated systems retained (no change due to medium),
- a gas of quasi-nucleons that contain self energy corrections, the clusters consist of quasi-nucleons but the interaction is without Pauli blocking, hence the binding energy will not change, and
- a gas of quasi-nucleons with Pauli blocking in the interaction and therefore the clusters are treated as quasi-nuclei that include the self energy corrections on the cluster level and dissociation.

In the ideal situation (case A), the components retain their properties, i.e. all particle masses stay the same. The composition of the system is driven by the law of mass action, i.e. the equilibrium distribution functions of nuclei (consisting of A nucleons) with mass $m_A = Am_N - B_A$ are given by

$$f_A(p) = \{\exp[\beta(p^2/2m_A - B_A - \mu_A)] + \epsilon\}^{-1}. \quad (29)$$

The composition of the system, i.e., the number of particles as a function of the total density, for $T = 10$ MeV is given in Fig. 4A. The density is accumulated by the more massive clusters the larger the total densities gets. The freeze-out distribution could be read off at $n_{\text{tot}} = 0.085 \dots 0.034 \text{ fm}^{-3}$ [11]. Fig. 4B refers to the result of the quasi-particle approximation (case B) for nucleons, instead of using ideal nucleons. In this case the medium effects are taken into account in Hartree-Fock approximation on the single particle level. This results in different self energies for the nucleon and in turn the mass of nuclei changes accordingly, see Eq. (4)

$$\varepsilon(k) \simeq k^2/2m^{\text{eff}} + \Sigma(0) \quad (30)$$

The right hand side of Eq. (30), known as effective mass approximation, is valid for the rather low momenta and

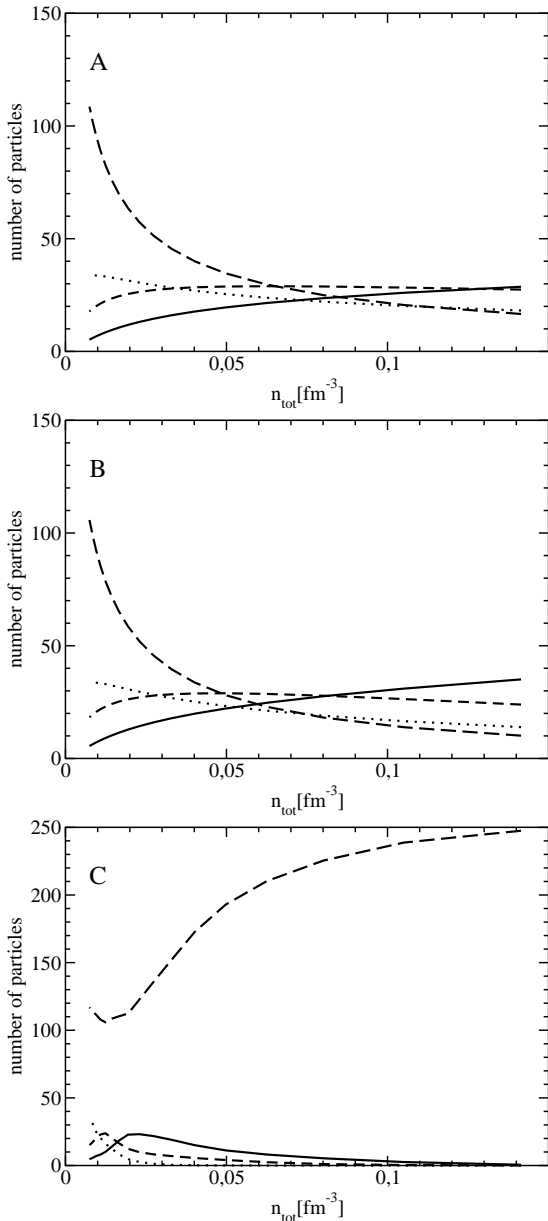


Fig. 4. Numbers of nucleon (long dashed), deuteron (dotted), triton (^3He) (dashed), ^4He (solid) as a function of the total density n_{tot} at $T = 10$ MeV. Total number of nucleons 250. A) ideal system B) quasi particle system, B) full calculation with dissociation.

densities considered, hence $m^{\text{eff}} = m_N(\mu, T)$ approximately independent of the momentum k . The distribution functions change to

$$f_A(p) = \{\exp[\beta(p^2/2m_A^{\text{eff}} - B_A - \mu_A^{\text{eff}})] + \epsilon\}^{-1} \quad (31)$$

and now $m_A^{\text{eff}} = Am_N^{\text{eff}} - B_A$. In chemical equilibrium $\mu_A^{\text{eff}} = A\mu^{\text{eff}} - \Sigma(0)$, where $\mu^{\text{eff}} = \mu - \Sigma(0)$. The results are rather close to the ideal gas case, because the change of the self energy of the cluster due to the binding energy of the bound nuclei is not taken into account. Differences appear at larger densities.

The situation changes drastically for case C, if the change of the binding energy as discussed above is taken into account,

$$B_A \rightarrow B_A(p, T, \mu) \equiv B_A^{\text{eff}}. \quad (32)$$

This, however, needs a solution of few-body in-medium equations as given in the previous section. The effects induced by this change in binding energy is shown in Fig. 4C. The equation for the density of the cluster changes, because the bound state exists only above the momentum of dissociation as shown in Fig. 2. The definition of the density changes accordingly, see Eq. (8)

$$n_A^{\text{b}}(\mu, T) = (2S + 1)(2I + 1) \sum_{p > p_{\text{dis}}} f_A(p). \quad (33)$$

Also the distribution function is different from the previous definition, since now the change of the binding energy has to be taken into account.

$$f_A(p) = \{\exp[\beta(p^2/2m_A^{\text{eff}} - B_A^{\text{eff}} - \mu_A^{\text{eff}})] + \epsilon\}^{-1} \quad (34)$$

where now $m_A^{\text{eff}} = Am_N(\mu, T) - B_A^{\text{eff}}$ and B_A^{eff} is given in Fig. 3 for the α -particle, for the three-body case in [16] and for the deuteron in [36], and Refs. therein.

The change between the ideal (or quasi-particle) picture and the full calculation that includes self energy corrections and dissociation of the clusters appears quite decisive. Whereas for rigid nuclei the number of heavy particles is much higher than the number of light particles, this is different, if the dissociation is taken into account. The geometrical interpretation of dissociation is because less low momentum components (large distance components) are available for the formation of a bound state. If the momentum is higher, the nucleus moves out of the Fermi sphere of the surrounding matter and the particle becomes more stable. The fact that no bound states are possible doesn't mean that there are no correlations. Previously we found by analyzing the Jost function of the deuteron that as the deuteron moves towards lower binding energies and eventually crosses the continuum line ($B_2 = 0$) it exists as a virtual bound state on the unphysical energy sheet [34]. In its turn this means that particular correlations in the continuum can form deuterons, if the density becomes low enough (for a given temperature). A similar study for three- and four-body states still needs to be done. On the other hand scattering states are infinitely extended, in contrast to bound states. So neglecting those few-body correlations related to scattering states may not be the worst approximation to start with.

To give an example for possible consequences of this finding, we investigate the multiplicities of light fragments in a heavy ion collision. We investigate conditions close to the INDRA experiment Xe on Sn at $50A$ MeV [9] studied earlier within the context of a BUU simulation [5]. We focus on the final stage of the collision and for simplicity assume a homogeneous temperature of $T = 10$ MeV that might slightly be too high for a quantitative comparison, but is still reasonable. Also, we use symmetric nuclear

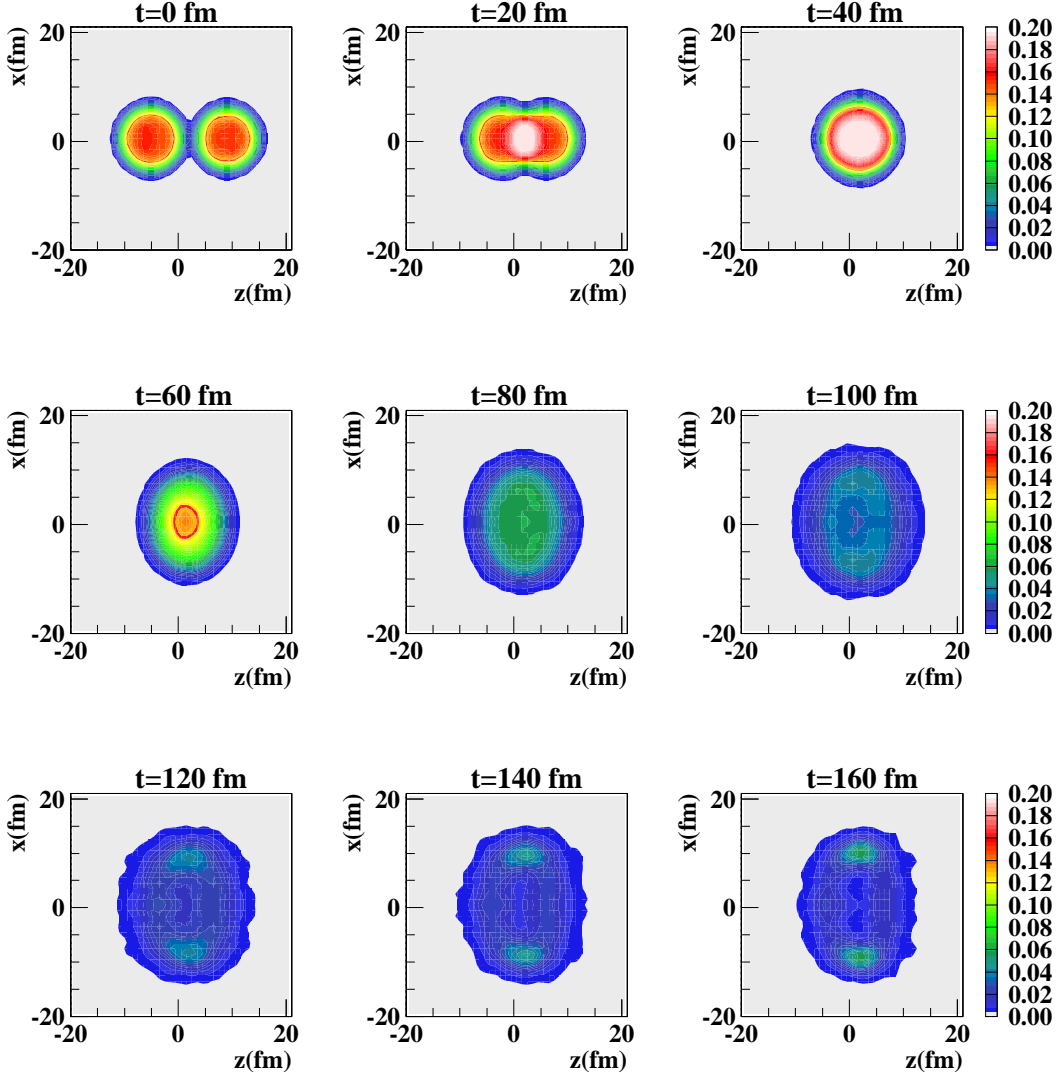


Fig. 5. Evolution of the density in the xz -plane as provided by a BUU simulation [18] of a central collision of Xe on Sn.

matter that is not achieved in the experiment mentioned. However, the basic effects that we focus on in this paper are not changed: We found previously that asymmetric nuclear matter (using the asymmetry induced by the experiment Xe on Sn) has very little effect on the dissociation of ^3He and triton. Quantitatively, this effect is in the same order of magnitude as the Coulomb correction [33].

The BUU simulation of the central collision of Xe on Sn at 50A MeV provides a realistic nuclear density distribution for the INDRA experiment. A cut through the xz -plane is shown in Fig. 5 [18]. To simplify and model this density distribution we assume a homogeneous spherical distribution of radius R that approximately matches the

size of the simulation at about 40 fm/c ($R = 7.5$ fm) and about 140 fm/c ($R = 20$ fm) after the collision. The radial change is assumed to be linear. The resulting change of the local density with respect to time for this simple expanding fire ball is shown in Fig. 6.

The multiplicities of nucleons, deuterons, $^3\text{He}/^3\text{H}$, and α -particles for the densities evolution of Fig. 6 and a temperature of $T = 10$ MeV for a total number of nucleons of 250 is given in Fig. 7. This is the main result of the present calculation.

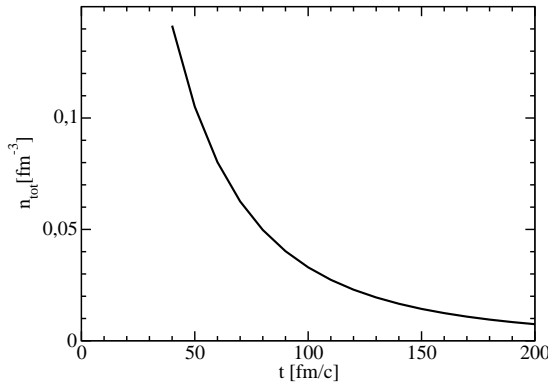


Fig. 6. Evolution of total density in a uniform model. Parameters are chosen as explained in the text.

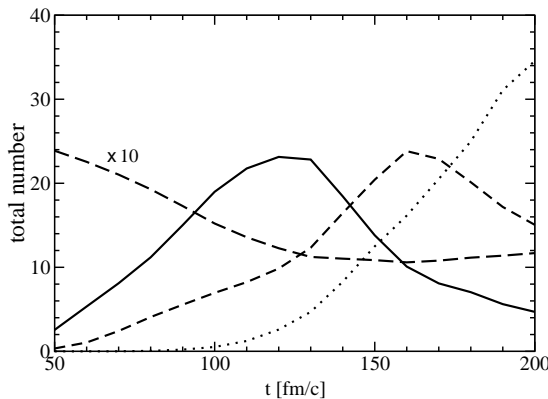


Fig. 7. Total numbers of nucleons (long-dashed $\times 10$), deuteron (dots), triton/³He (dashed), and α particles (solid) as a function of collision time at $T = 10$ MeV.

4.3 Discussion

At around $t = 100$ fm/c the number of α -particles is much larger than the number of other clusters. This time, which (approximately) corresponds to about 3-4 times the initial volume, can be considered as freeze-out time (related to the freeze-out volume [10]). Hence the multiplicities at this time should be significantly correlated with the experimentally observed ones. Indeed, the total multiplicities of α -particles in the above mentioned INDRA experiments Xe+Sn is larger than those of the lighter clusters [10].

In contrast to the full calculation, the other equilibrium scenarios discussed above have the opposite ordering of multiplicities which can be concluded from Fig. 4 for $n_{\text{tot}} \simeq 0.04 \text{ fm}^{-3}$ and does not reflect the experimental finding for the large excess of α -particles. We argue that the enhancement of α -particles is also related to the fact that the α -particle is more stable in low density nuclear matter than the other light clusters. Our findings of the ordering of multiplicities for the light fragments obtained via a microscopic approach and including dissociation might provide a natural explanation to the excess of α -particles. However, for a throughout comparison with experimental data several other aspects have to be taken into account

as mentioned in [10, 13]. However, some of them need a major effort while going beyond the model of an ideal gas of components.

Concerning larger (light) clusters than the ones considered so far, note that they are weaker bound than the α -particle. Therefore they should be less stable in medium. Hence, at freeze-out their multiplicity should be smaller than that of the α -particle. However, a more quantitative analysis is certainly needed. Within the equilibrium scenario the most stable nucleus might be Fe. However, little is known about the properties of Fe at finite temperature. At low densities one might expect a linear dependence of the binding energy (perturbative theory), however the calculation for the α -particle clearly shows that this might not be valid for a stronger bound system. On the other hand during (central) heavy ion collision the dynamical generation of heavy nuclei needs time due to many (binary) collisions in the system and such heavy elements might not recombine at all in such a evaporation scenario [12].

A microscopic treatment of more complex (light) nuclei could be achieved, e.g., along the lines of [37]. So far, larger and heavier clusters are "hidden" in the large number of nucleons present. While those are rather easy to incorporate in the ideal gas picture, a calculation including medium dependence such as self energy corrections and Pauli blocking is more elaborate.

5 Conclusion

We have shown that a systematic microscopic calculation provides strong changes in the equilibrium composition of clusters in nuclear matter. The changes are strong enough to invert the ordering of multiplicities at freeze-out compared to the ideal case. Therefore an explanation of experimental results in terms of a microscopic picture with realistic nucleon nucleon forces evaluated in an equilibrium scenario might be possible. Note that a detailed comparison of this approach to the experimental data as, e.g., given by the INDRA collaboration for the SMM [9, 10], needs much further investigation and has to be postponed to a future communication.

Acknowledgment: We thank Christiane Kuhrt for providing us with Fig. 5 [18] and Gerd Röpke for discussions. MB acknowledges the warm hospitality of the IPN Groupe Théorie and the Physics Department of UNISA during longer research stays. Work supported by Deutsche Forschungsgemeinschaft BE 1092/7.

References

1. P. Danielewicz and G.F. Bertsch, Nucl. Phys. **A533**, 712 (1991).
2. P. Danielewicz and Q. Pan, Phys. Rev. C **46**, 2002 (1992).
3. H. Stöcker and W. Greiner, Phys. Rep. **137**, 277 (1986).
4. C. Fuchs and H.H. Wolter, Nucl. Phys. **A589**, 732 (1995).
5. M. Beyer, C. Kuhrt, G. Röpke and P. D. Danielewicz, Phys. Rev. C **63**, 034605 (2001).

6. J. Aichelin, Phys. Rep. **202**, 233 (1991).
7. G. Peilert *et al.*, Phys. Rev. C **46**, 1457 (1992).
8. R. Nebauer and J. Aichelin, Nucl. Phys. **A650**, 65 (1999); INDRA Collaboration, R. Nebauer *et al.*, Nucl. Phys. A658, 67 (1999).
9. INDRA Collaboration, D. Gorio *et al.*, Eur. Phys. J. A **7**, 245 (2000), and references therein.
10. INDRA Collaboration, S. Hudan *et al.*, Phys. Rev. C **67**, 064613 (2003).
11. INDRA Collaboration, B. Borderie *et al.*, Phys. Lett. B **388**, 224 (1996).
12. INDRA Collaboration, B. Borderie *et al.*, Phys. Lett. B **353**, 27 (1995).
13. A.Z. Mekjian, Phys. Rev. C **17**, 1051 (1978).
14. R.K. Tripathi and L.W. Townsend, Phys. Rev. C **50**, R7 (1994).
15. J.P. Bondorf, A.S. Botvina, A.S. Iljinov, I.N. Mishustin, and K. Sneppen, Phys. Rept. **257**, 133 (1995).
16. M. Beyer, W. Schadow, C. Kuhrt, and G. Röpke, Phys. Rev. C **60**, 034004 (1999).
17. M. Beyer, S. A. Sofianos, C. Kuhrt, G. Röpke and P. Schuck, Phys. Lett. **B488**, 247 (2000).
18. Chr. Kuhrt, *PhD thesis: "Deuteron production in heavy ion reactions"* Rostock 2000.
19. For a textbook treatment see, e.g., L.P. Kadanoff, G. Baym, *Quantum Theory of Many-Particle Systems* (Mc Graw-Hill, New York, 1962); A.L. Fetter, J.D. Walecka, *Quantum Theory of Many-Particle Systems*, (Mc Graw-Hill, New York, 1971).
20. see e.g., J. Dukelsky, G. Röpke, and P. Schuck, Nucl. Phys. A **628**, 17 (1998).
21. M. Beyer, G. Röpke, and A. Sedrakian, Phys. Let. B **376**, 7 (1996).
22. H.A. Bethe and J. Goldstone, Proc. R. Soc. A **238**, 551 (1957).
23. J. Eichler, T. Marumori, and K. Takada, Prog. Theor. Phys. **40**, 60 (1968).
24. P. Schuck, F. Villars, and P. Ring, Nucl. Phys. A **208**, 302 (1973).
25. M. Schmidt, G. Röpke, H. Schulz, Ann. Phys. (N.Y.) bf 202, 57 (1990).
26. E.O. Alt, P. Grassberger, W. Sandhas, Nucl. Phys. B **2** (1967) 167.
27. W. Sandhas, Acta Physica Austriaca, Suppl. **XIII**, 679 (1974).
28. E.O. Alt, P. Grassberger and W. Sandhas, Report E4-6688, JINR, Dubna 1972 and in *Few particle problems in the nuclear interaction* eds. I. Slaus et al. (North Holland, Amsterdam 1972) p. 299.
29. W. Sandhas, Czech. J. Phys. B **25**, 251 (1975).
30. S. Sofianos, N.J. McGurk, and H. Fiedeldey, Nucl. Phys. A**318**, 295 (1979); S.A. Sofianos, H. Fiedeldey, H. Haberzettl, and W. Sandhas Phys. Rev. C **26**, 228 (1982).
31. Y. Yamaguchi, Phys. Rev. **95**, 1628 (1954).
32. R.A. Malfliet and J. Tjon, Nucl. Phys. bf A 127, 161 (1969).
33. S. Mattiello, *diploma thesis: "Production of three-body clusters in asymmetric matter" (in Italian)*, U. Trento 2000 (unpublished).
34. M. Beyer and S. A. Sofianos, J. Phys. G **27**, 2081 (2001).
35. Efimov, V. N., Yad. Fiz **12**, 1080 (1970) [Sov. J. Nuc. Phys. **12**, 589 (1971)].
36. A. Schnell, *PhD thesis*, U. Rostock 1999.
37. S.A. Sofianos, 17th International Few-Body Conference (2003).